Separation Science and Technology
Publication details, including instructions for authors and subscription information:
http://www.informaworld.com/smpp/title~content=t713708471

Analysis of Membrane Separation Parameters. II. Counter-current and Cocurrent Flow in a Single Permeation Stage

W. P. Walawender[a]; S. A. Stern[b]
[a] DEPARTMENT OF CHEMICAL ENGINEERING, KANSAS STATE UNIVERSITY, MANHATTAN, KANSAS [b] DEPARTMENT OF CHEMICAL ENGINEERING AND MATERIALS SCIENCE, SYRACUSE UNIVERSITY, SYRACUSE, NEW YORK

To cite this Article Walawender, W. P. and Stern, S. A.(1972) 'Analysis of Membrane Separation Parameters. II. Counter-current and Cocurrent Flow in a Single Permeation Stage', Separation Science and Technology, 7: 5, 553 — 584
To link to this Article: DOI: 10.1080/00372367208056054
URL: http://dx.doi.org/10.1080/00372367208056054

SEPARATION SCIENCE, 7(5), pp. 553–584, 1972

Analysis of Membrane Separation Parameters. II. Countercurrent and Cocurrent Flow in a Single Permeation Stage

W. P. WALAWENDER

DEPARTMENT OF CHEMICAL ENGINEERING
KANSAS STATE UNIVERSITY
MANHATTAN, KANSAS 66506

S. A. STERN*

DEPARTMENT OF CHEMICAL ENGINEERING AND MATERIALS SCIENCE
SYRACUSE UNIVERSITY
SYRACUSE, NEW YORK 13210

Abstract

Analytical expressions are presented for calculating the extent of separation of binary gas mixtures achievable in a permeation stage, as well as the required membrane area, when the high- and low-pressure streams in the stage flow either countercurrently or cocurrently to each other. The derivations are similar to those of Oishi et al., but are cast in a form suitable for computer calculations. The results of a parametric study on the separation of oxygen from air are presented for four different flow patterns inside the stage: (a) countercurrent flow, (b) cocurrent flow, (c) cross-flow, and (d) perfect mixing. In the first three cases it is assumed that no mixing occurs on the two sides of the stage (or membrane). The type of flow in the permeation stage can have a significant effect on the degree of separation, but has relatively little effect on the membrane area at low separation factors. Countercurrent flow is the most efficient flow pattern, whereas perfect mixing is the least efficient one, both from the viewpoints of extent of separation and membrane area requirements.

* To whom correspondence should be addressed.

INTRODUCTION

The separation of gases by selective permeation through nonporous polymeric membranes is a research field of continuing interest because of its potentially important applications in industry and biomedicine. The development of gas permeation processes requires a detailed knowledge of the relations among the parameters affecting the operation of the permeation stage, which is the basic building block of such processes. For a given gas mixture and membrane, these parameters include: the feed rate and composition, the pressure on the two sides of the membrane, the temperature, the fraction of the feed allowed to permeate (the "stage cut"), and the flow patterns of the permeated and unpermeated streams in the stage. An analysis of the listed parameters and their interactions will yield information on the degree of separation achievable in a permeation stage and the corresponding membrane area requirements. Such an analysis will determine the optimum operating conditions and stage design and, therefore, the minimum power and capital investment costs of the process. The analysis of separation parameters is more complicated in the case of a multistage, or cascade, process, but the principles of cascade design are well established (*1*).

The separation of gases in a single stage was first studied analytically by Weller (*2*, *3*), who examined the effect of two limiting flow patterns for the permeated and unpermeated streams in the stage: (a) flow with perfect mixing, and (b) cross-flow with no mixing. Weller's study was limited to binary mixtures, but the perfect mixing case was extended by Kammermeyer and his associates (*4*, *5*) to ternary and quaternary mixtures. An alternative derivation for cross-flow with no mixing was given by Naylor and Backer (*6*) for the separation of binary mixtures, while Breuer and Kammermeyer (*7*) studied the effect of concentration gradients on this type of flow pattern. Stern, Vahldieck, et al. (*8*) reported an iterative computation method applicable to both types of flow patterns and particularly useful for calculations involving multicomponent mixtures. Finally, the present authors critically reviewed all previous work and described computer programs for parametric studies (*9*).

The present work extends the analysis of membrane separation parameters to two other important flow patterns in a single stage, namely, cocurrent and countercurrent flow of the permeated and unpermeated streams along the membrane. These cases have been studied

previously only by Oishi et al. (*10*) for the gaseous diffusion of binary mixtures across *porous* barriers. The analysis of these investigators can be applied also to nonporous barriers, such as polymeric membranes, but their results are expressed in terms of dimensionless groups which do not provide a direct comparison with previous work. The study of Oishi et al. is reviewed here in some detail and is cast in a form suitable for computer calculations. The four types of stage flow patterns mentioned above are then compared to each other, with reference to an important process, namely, the separation of oxygen from air.

ANALYTICAL STUDIES

Cocurrent Flow

This case is shown schematically in Fig. 1, which is a diagram of a permeation stage. As indicated, the stage is divided into two sections by a nonporous membrane. A binary mixture of gaseous Components A and B is introduced as feed at a total pressure p_h and molar feed rate $L_{i(h)}$, where the subscript "i" stands for "inlet" and the subscript h indicates the high-pressure side of the barrier; the mole fraction of the more permeable component, assumed to be A, is denoted x_i^A. The pressure is held constant throughout the high-pressure side of the barrier, and a specified fraction of the feed, θ, is allowed to permeate through the membrane into the second section of the stage which is maintained at a lower pressure p_l. The subscript l refers to this second section. The gas streams on each side of the barrier flow parallel to the barrier and in the same direction. It is assumed that no mixing occurs in either stream, i.e., no concentration gradients exist in the direct u perpendicular to the membrane. Therefore, the composition of the gas streams on each side of the barrier at any point v depends only on the amount of fluid permeated. The feed stream is separated into a permeated stream enriched in Component A and an unpermeated stream which is depleted in this component. When leaving the stage, the molar flow rates of these streams are $L_{o(l)}$ and $L_{o(h)}$, respectively, and the corresponding mole fractions of A in the streams are y_o^A and x_o^A. The subscript "o" stands for "outlet." The mole fraction y_o^A is also referred to as the "enrichment."

Reference is made to a differential volume element on the high pressure side of the barrier, as indicated in Fig. 1. The *local* molar flux of Component A out of this element and into the low-pressure side of the

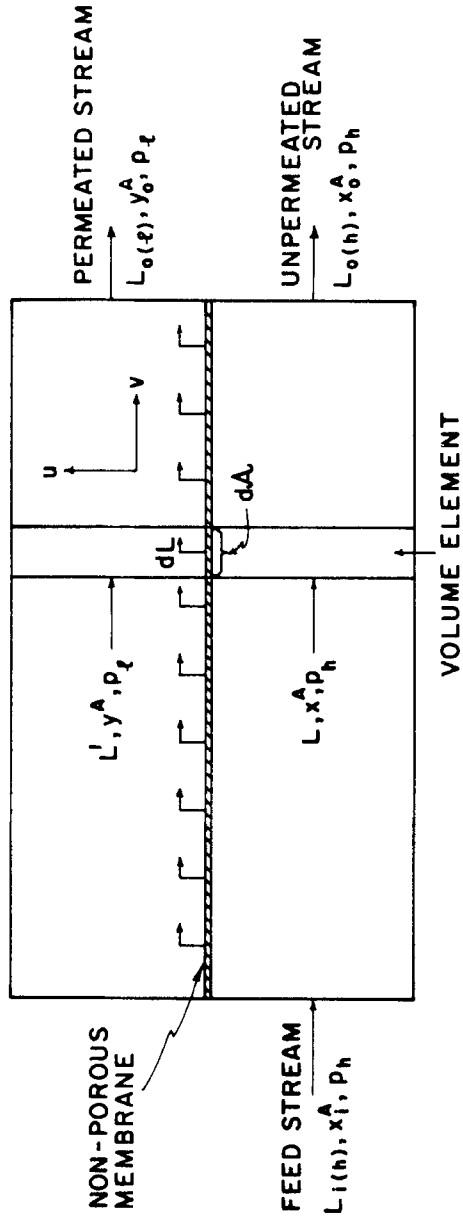

FIG. 1. Diagram of single permeation stage with cocurrent flow.

membrane can be expressed by Fick's law:

$$-y^A dL = \left(\frac{P^A}{\delta}\right)(p_h x^A - p_l y^A)\, d\mathcal{A} \tag{1}$$

where x^A and y^A represent the *local* compositions of Component A in the high- and low-pressure streams, respectively; $d\mathcal{A}$ is the membrane surface area of the element and dL is the increment of the local high-pressure stream permeated through that area; P^A is the permeability coefficient for pure Component A; and δ is the membrane thickness.

The expression for the local molar flux applies only with the following restrictions:

(1) The gases permeate by activated diffusion through the membrane matrix, with solution equilibrium for the penetrants established at the two membrane interfaces (*11*). This is sometimes referred to as the "solution-diffusion" mechanism.

(2) There is no interaction between the permeating components of the mixture, i.e., each gas permeates independently of the other. Hence, the permeability coefficient for each component of the mixture is the same as that for the pure component.

(3) The transport of gas across the membrane is at steady-state.

(4) The permeability coefficients are independent of pressure, and depend only on the nature of the gas-membrane system and the temperature.

In addition to Eq. (1), several material balances are available. Thus, at any point v in the stage downstream from the inlet, it is possible to write the overall balance

$$L_{i(h)} = L + L' \tag{2}$$

where L and L' are the *local* molar flow rates of the unpermeated (high-pressure) and permeated (low-pressure) streams, respectively. The corresponding material balance for Component A is then

$$L_{i(h)} x_i^A = L x^A + L' y^A \tag{3}$$

Differentiating Eq. (3) shows that

$$d(L' y^A) = -d(L x^A) \tag{4}$$

A material balance is now written about a differential volume element on the high-pressure side of the barrier, as shown in Fig. 2. This balance

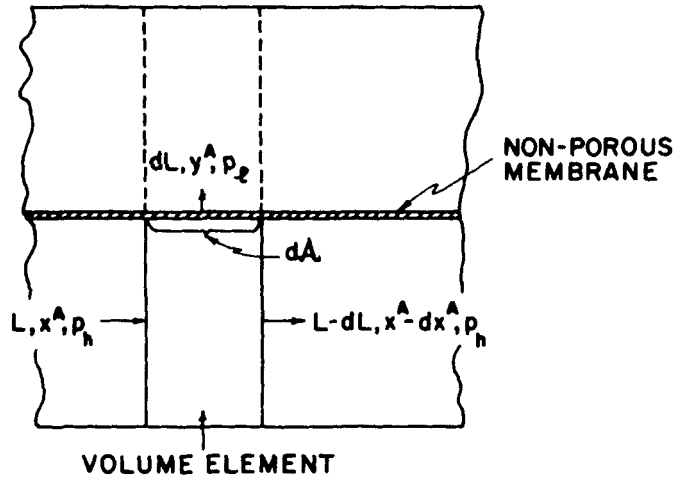

FIG. 2. Differential volume element on high-pressure side of stage.

reduces to

$$y^A\,dL = L\,dx^A + x^A\,dL = d(Lx^A) \tag{5}$$

where second-order differentials have been neglected.

Combining Eqs. (1), (4), and (5) yields for Component A

$$-d(Lx^A) = d(L'y^A) = \left(\frac{P^A}{\delta}\right)(p_h x^A - p_l y^A)\,d\mathcal{A} \tag{6}$$

Similarly for Component B:

$$-d[L(1-x^A)] = d[L'(1-y^A)]$$
$$= (P^B/\delta)[p_h(1-x^A) - p_l(1-y^A)]\,d\mathcal{A} \tag{7}$$

Substitution of L' from Eq. (2) into Eq. (3), followed by rearrangement and multiplication by dx^A, yields

$$L_{i(h)}\,dx^A = \left(\frac{x^A - y^A}{y^A - x_i{}^A}\right)(-L\,dx^A) \tag{8}$$

It can be shown that

$$-L\,dx^A = -(1-x^A)\,d(Lx^A) + x^A\,d[L(1-x^A)] \tag{9}$$

Substitution of Eq. (9) in Eq. (8), followed by substitution of Eqs. (6) and (7), results in the expression

$$L_{i(h)} \frac{dx^A}{d\mathcal{Q}} = \left(\frac{x^A - y^A}{y^A - x_i{}^A}\right) \{(1 - x^A)(P^A/\delta)(p_h x^A - p_l y^A) - x^A(P^B/\delta)[p_h(1 - x^A) - p_l(1 - y^A)]\} \quad (10)$$

A similar expression can be obtained for $L_{i(h)}(dy^A/d\mathcal{Q})$ as follows. Substitution of L from Eq. (2) into Eq. (3), followed by rearrangement and multiplication by dy^A, gives

$$L_{i(h)}\, dy^A = \left(\frac{x^A - y^A}{x^A - x_i{}^A}\right)(L'\, dy^A) \quad (11)$$

It can also be shown that

$$L'\, dy^A = (1 - y^A)\, d(L'y^A) - y^A\, d[L'(1 - y^A)] \quad (12)$$

Substitution of Eq. (12) into Eq. (11), followed by substitution of Eqs. (6) and (7), results in the expression:

$$L_{i(h)} \frac{dy^A}{d\mathcal{Q}} = \left(\frac{x^A - y^A}{x^A - x_i{}^A}\right) \{(1 - y^A)(P^A/\delta)(p_h x^A - p_l y^A) - y^A(P^B/\delta)[p_h(1 - x^A) - p_l(1 - y^A)]\} \quad (13)$$

Equations (10) and (13) have been derived in a similar form by Oishi et al. (*10*). These equations can be expressed in a more compact form by introducing the ideal separation factor α^* and the pressure ratio r, which are defined by

$$\alpha^* = P^A/P^B \quad (14)$$

and

$$r = p_h/p_l \quad (15)$$

In terms of α^* and r, Eqs. (10) and (13) take the form

$$K \frac{dx^A}{d\mathcal{Q}} = \left(\frac{x^A - y^A}{y^A - x_i{}^A}\right) \{(1 - x^A)\alpha^*(rx^A - y^A) - x^A[r(1 - x^A) - (1 - y^A)]\} \quad (16)$$

and

$$K\frac{dy^A}{d\mathfrak{A}} = \left(\frac{x^A - y^A}{x^A - x_i{}^A}\right)\{(1 - y^A)\alpha^*(rx^A - y^A) - y^A[r(1 - x^A) - (1 - y^A)]\} \quad (17)$$

where

$$K = [L_{i(h)}\delta]/p_i P^B \quad (18)$$

Equations (16) and (17) can be solved simultaneously by numerical methods, provided that the conditions at the stage inlet are available. These conditions are:

$$\mathfrak{A} = 0; \qquad x^A = x_i{}^A; \qquad \text{and} \qquad y^A = y_i{}^A$$

The value of $x_i{}^A$ is known, but that of $y_i{}^A$ is not. The latter can be evaluated by the following procedure. The ratio of Eqs. (6) and (7) is first taken and yields:

$$\frac{d(L'y^A)}{d[L'(1 - y^A)]} = \frac{\alpha^*(rx^A - y^A)}{r(1 - x^A) - (1 - y^A)} \quad (19)$$

Evaluation of Eq. (12) at the stage inlet, noting that at this place in the stage $L' = 0$, yields

$$\left.\frac{d(L'y^A)}{d[L'(1 - y^A)]}\right|_{y^A = y_i{}^A} = \frac{y_i{}^A}{1 - y_i{}^A} \quad (20)$$

Substitution of this result into Eq. (19) for the inlet conditions gives

$$\frac{y_i{}^A}{1 - y_i{}^A} = \frac{\alpha^*(rx_i{}^A - y_i{}^A)}{r(1 - x_i{}^A) - (1 - y_i{}^A)} \quad (21)$$

Finally, Eq. (21) can be expressed as a quadratic in $y_i{}^A$ and solved for $y_i{}^A$ to give

$$y_i{}^A = \frac{(\alpha^* - 1)(rx_i{}^A + 1) + r - \{[(\alpha^* - 1)(rx_i{}^A + 1) + r]^2 - 4\alpha^* rx_i{}^A(\alpha^* - 1)\}^{1/2}}{2(\alpha^* - 1)} \quad (22)$$

It should be noted that in Eq. (22) only the negative root is physically meaningful.

Inspection of Eq. (17) (in conjunction with Eq. 21) reveals that it is indeterminate at the stage inlet; application of L'Hôpital's rule as

$\mathcal{A} \rightarrow 0$ gives:

$$\left(\frac{dy^A}{d\mathcal{A}}\right)\Big|_{\mathcal{A}=0}$$

$$= \frac{(x_i{}^A - y_i{}^A)r[\alpha^* - y_i{}^A(\alpha^* - 1)]}{K - \{(x_i{}^A - y_i{}^A)[(\alpha^* - 1)(2y_i{}^A - rx_i{}^A - 1) - r]\}/(dx^A/d\mathcal{A})\ |_{\mathcal{A}=0}} \tag{23}$$

The value of $(dx^A/d\mathcal{A})\ |_{\mathcal{A}=0}$ can be readily obtained from Eq. (16):

$$\left(\frac{dx^A}{d\mathcal{A}}\right)\Big|_{\mathcal{A}=0} = \frac{1}{K}\left[\frac{\alpha^*(rx_i{}^A - y_i{}^A)(x_i{}^A - y_i{}^A)}{y_i{}^A}\right] \tag{24}$$

It is perhaps more convenient to solve Eqs. (16) and (17) with y^A as the independent variable. The necessary expressions can be obtained as follows. Division of Eq. (16) by Eq. (17) yields:

$$\frac{dx^A}{dy^A} = \left(\frac{x^A - x_i{}^A}{y^A - x_i{}^A}\right)$$

$$\times \left\{\frac{(1 - x^A)\alpha^*(rx^A - y^A) - x^A[r(1 - x^A) - (1 - y^A)]}{(1 - y^A)\alpha^*(rx^A - y^A) - y^A[r(1 - x^A) - (1 - y^A)]}\right\} \tag{25}$$

and inversion of Eq. (17) gives:

$$\frac{d\mathcal{A}}{dy^A} = \frac{K[(x^A - x_i{}^A)/(x^A - y^A)]}{(1 - y^A)\alpha^*(rx^A - y^A) - y^A[r(1 - x^A) - (1 - y^A)]} \tag{26}$$

Both Eqs. (25) and (26) are indeterminate at the inlet, but can be evaluated at that point with the aid of Eqs. (23) and (24):

$$\left(\frac{dx^A}{dy^A}\right)\Big|_{\mathcal{A}=0} = \left(\frac{dx^A}{d\mathcal{A}}\right)\Big|_{\mathcal{A}=0} \Big/ \left(\frac{dy^A}{d\mathcal{A}}\right)\Big|_{\mathcal{A}=0} \tag{27}$$

$$\left(\frac{d\mathcal{A}}{dy^A}\right)\Big|_{\mathcal{A}=0} = 1 \Big/ \left(\frac{dy^A}{d\mathcal{A}}\right)\Big|_{\mathcal{A}=0} \tag{28}$$

Equations (25) and (26) can be solved simultaneously to evaluate $x_o{}^A$, $y_o{}^A$, and the membrane area requirement. With this information, $L_{o(l)}$ and $L_{o(h)}$ can be evaluated with the aid of the material balances, Eqs. (2) and (3), by replacing L and L' with $L_{o(h)}$ and $L_{o(l)}$, respectively.

The "stage cut," or fraction of feed permeated, θ, can then be evaluated from:

$$\theta = L_{o(l)}/L_{i(h)} = (x_i{}^A - x^A)/(y^A - x^A) \tag{29}$$

Countercurrent Flow

Countercurrent flow in a permeation stage is illustrated in Fig. 3. From an analytical viewpoint, this case is similar to that of cocurrent flow, with the obvious exception that the high-pressure (unpermeated) and low-pressure (permeated) streams flow in opposite directions along the membrane.

The molar flux of Component A out of a differential volume element on the high-pressure side of the membrane is again given by Eq. (1). The overall material balance is

$$L = L_{o(h)} + L' \tag{30}$$

and the material balance for Component A is

$$Lx^A = L_{o(h)}x_o{}^A + L'y^A \tag{31}$$

Differentiating Eq. (31) shows that

$$d(Lx^A) = d(L'y^A) \tag{32}$$

Equation (5) for the differential volume element applies also in the case of countercurrent flow. The combination of Eqs. (1), (5), and (32) yields the following relation for Component A:

$$-d(L'y^A) = -d(Lx^A) = (P^A/\delta)(p_hx^A - p_ly^A)\, d\mathcal{A} \tag{33}$$

Similarly, for Component B:

$$\begin{aligned} -d[L'(1 - y^A)] &= -d[L(1 - x^A)] \\ &= (P^B/\delta)[p_h(1 - x^A) - p_l(1 - y^A)]d\mathcal{A} \end{aligned} \tag{34}$$

Substitution of L' from Eq. (30) into Eq. (31), followed by rearrangement and multiplication by dx^A, gives

$$L_{o(h)}\, dx^A = \left(\frac{x^A - y^A}{y^A - x_o{}^A}\right)(-L\, dx^A) \tag{35}$$

Next, substitution of the expression for $(-L\, dx^A)$ from Eq. (9) into Eq. (35), followed by the substitution of Eqs. (33) and (34), gives

$$\begin{aligned} L_{o(h)}\frac{dx^A}{d\mathcal{A}} = \left(\frac{x^A - y^A}{y^A - x_o{}^A}\right)\{&(1 - x^A)(P^A/\delta)(p_hx^A - p_ly^A) \\ &- x^A(P^B/\delta)[p_h(1 - x^A) - p_l(1 - y^A)]\} \end{aligned} \tag{36}$$

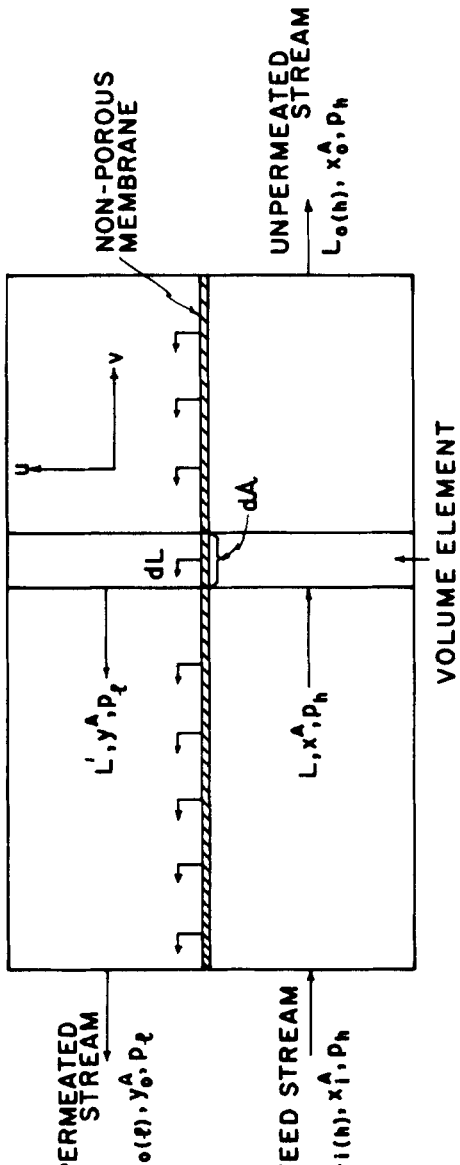

FIG. 3. Diagram of single permeation stage with countercurrent flow.

A similar expression for $L_{o(h)}(dy^A/d\mathcal{A})$ can be obtained as follows. Substitution of L from Eq. (30) into Eq. (31), followed by rearrangement and multiplication by dy^A, gives

$$L_{o(h)}\, dy^A = \left(\frac{x^A - y^A}{x^A - x_o{}^A}\right)(-L'\, dy^A) \tag{37}$$

Then substitution for $(L'\, dy^A)$ from Eq. (12) into Eq. (37), followed by substitution of Eqs. (33) and (34), results in the expression

$$L_{o(h)}\frac{dy^A}{d\mathcal{A}} = \left(\frac{x^A - y^A}{x^A - x_o{}^A}\right)\{(1 - y^A)(P^A/\delta)(p_h x^A - p_l y^A) - y^A(P^B/\delta)[p_h(1 - x^A) - p_l(1 - y^A)]\} \tag{38}$$

Equations (36) and (38) can be expressed in terms of α^* and r, which are defined by Eqs. (14) and (15), respectively. Equation (36) then becomes

$$K'\frac{dx^A}{d\mathcal{A}} = \left(\frac{x^A - y^A}{y^A - x_o{}^A}\right)\{(1 - x^A)\alpha^*(rx^A - y^A) - x^A[r(1 - x^A) - (1 - y^A)]\} \tag{39}$$

while Eq. (38) takes the form

$$K'\frac{dy^A}{d\mathcal{A}} = \left(\frac{x^A - y^A}{x^A - x_o{}^A}\right)\{(1 - y^A)\alpha^*(rx^A - y^A) - y^A[r(1 - x^A) - (1 - y^A)]\} \tag{40}$$

where

$$K' = L_{o(h)}\delta/p_l P^B \tag{41}$$

Equations (39) and (40) have been derived in a slightly different form by Oishi et al. These equations are similar to Eqs. (16) and (17) for cocurrent flow and differ from the latter only in that $x_o{}^A$ and $L_{o(h)}$ are in place of $x_i{}^A$ and $L_{i(h)}$, respectively.

Equations (39) and (40) can be solved simultaneously by numerical methods if the stage outlet of the high-pressure (unpermeated) stream is taken as reference for the computations. Since $x_o{}^A$ will be generally unknown, a trial-and-error method must be employed along with the numerical solution. At the high-pressure outlet, $x = x_o{}^A$, $y = y_i{}^A$, while the value of $\mathcal{A}$ is unknown. If $\mathcal{A}$ is arbitrarily set equal to zero at that outlet, negative areas will be obtained from the numerical solution; the sign of $\mathcal{A}$ must then be reversed.

The procedure for solution is to *assume* a value for x_o^A, calculate y_o^A from the differential equations, and, with the aid of y_o^A, calculate x_o^A by material balance. If the x_o^A obtained from the material balance does not agree with the assumed value, a new value is selected for x_o^A and the above procedure is repeated until agreement is obtained.

The value for y_i^A can be obtained as follows. Evaluation of Eq. (12) at the high-pressure stage outlet results in an expression which is identical with Eq. (20). Substitution of this result in Eq. (19) for the outlet conditions gives

$$\frac{y_i^A}{1 - y_i^A} = \frac{\alpha^*(rx_o^A - y_i^A)}{r(1 - x_o^A) - (1 - y_i^A)} \tag{42}$$

Equation (42) can be expressed as a quadratic in y_i^A and solved for y_i^A to yield

$$y_i^A = \frac{(\alpha^* - 1)(rx_o^A + 1) + r - \{[(\alpha^* - 1)(rx_o^A + 1) + r]^2 - 4\alpha^* rx_o^A(\alpha^* - 1)\}^{1/2}}{2(\alpha^* - 1)} \tag{43}$$

Inspection of Eq. (40), in conjunction with Eq. (42), shows that it is indeterminate at the high-pressure stage outlet. This difficulty can be resolved as in the cocurrent case by applying L'Hôpital's rule for $\mathcal{A}$ (the arbitrary area) $\rightarrow 0$. This operation results in the expression:

$$\left(\frac{dy^A}{d\mathcal{A}}\right)\Bigg|_{\mathcal{A}=0} = \frac{(x_o^A - y_i^A)r[\alpha^* - y_i^A(\alpha^* - 1)]}{K' - \{(x_o^A - y_i^A)[(\alpha^* - 1)(2y_i^A - rx_o^A - 1) - r]\}/(dx^A/d\mathcal{A})\ |_{\mathcal{A}=0}} \tag{44}$$

The value of $(dx^A/d\mathcal{A})\ |_{\mathcal{A}=0}$ can be readily obtained from Eq. (39):

$$\left(\frac{dx^A}{d\mathcal{A}}\right)\Bigg|_{\mathcal{A}=0} = \frac{1}{K'}\left[\frac{\alpha^*(rx_o^A - y_i^A)(x_o^A - y_i^A)}{y_i^A}\right] \tag{45}$$

It is more convenient to solve Eqs. (39) and (40) in terms of x^A as the independent variable. The necessary relations are obtained as

follows. Division of Eq. (40) by Eq. (39) gives

$$\frac{dy^A}{dx^A} = \left(\frac{y^A - x_o{}^A}{x^A - x_o{}^A}\right) \times \left\{\frac{(1 - y^A)\alpha^*(rx^A - y^A) - y^A[r(1 - x^A) - (1 - y^A)]}{(1 - x^A)\alpha^*(rx^A - y^A) - x^A[r(1 - x^A) - (1 - y^A)]}\right\} \quad (46)$$

and inversion of Eq. (39) gives

$$\frac{d\mathcal{A}}{dx^A} = \frac{K'[(y^A - x_o{}^A)/(x^A - y^A)]}{(1 - x^A)\alpha^*(rx^A - y^A) - x^A[r(1 - x^A) - (1 - y^A)]} \quad (47)$$

Equation (46) is indeterminate at the high-pressure stage outlet, but can be evaluated at that point with the aid of Eqs. (44) and (45):

$$\left(\frac{dy^A}{dx^A}\right)\Bigg|_{\mathcal{A}=0} = \left(\frac{dy^A}{d\mathcal{A}}\right)\Bigg|_{\mathcal{A}=0} \Bigg/ \left(\frac{dx^A}{d\mathcal{A}}\right)\Bigg|_{\mathcal{A}=0} \quad (48)$$

Equations (46) and (47) can be solved simultaneously for each trial value of $x_o{}^A$ to evaluate $y_o{}^A$ and $\mathcal{A}$. In this calculation, the "stage cut" θ must be specified in order to obtain a value of $L_{o(h)}$:

$$L_{o(h)} = L_{i(l)}(1 - \theta) \quad (49)$$

This procedure is perhaps more convenient than specifying $L_{o(h)}$ directly.

COMPUTER PROGRAMS

Computer programs were written to calculate the composition of product streams and the membrane area for the two flow patterns discussed above. These programs were used for a parametric study of the separation of oxygen from air under conditions outlined in the following section. The computations were performed with the aid of an IBM 360/50 computer. A description of the programs follows.

Cocurrent Flow

The IBM System/360 Continuous System Modeling Program (CSMP) was employed in this case. CSMP is designed for the solution of differential equations for which the initial condition is zero for the independent variable (*11*). In order to apply this method to the solution

of Eqs. (25) and (26), the following change of variable must be made:

$$z = y_i^A - y^A \tag{50}$$

Substitution of this variable into Eqs. (25) and (26) results in

$$\frac{dx^A}{dz} = \left(\frac{x_i^A - x^A}{y_i^A - z - x_i^A}\right)\left\{\frac{(1-x^A)\alpha^*(rx^A + z - y_i^A) - x^A[r(1-x^A) - (1+z-y_i^A)]}{(1+z-y_i^A)\alpha^*(rx^A+z-y_i^A) + (z-y_i^A)[r(1-x^A) - (1+z-y_i^A)]}\right\} \tag{51}$$

and

$$\frac{d\mathcal{A}}{dz} = \frac{K[(x_i^A - x^A)/(x^A + z - y_i^A)]}{(1+z-y_i^A)\alpha^*(rx^A+z-y_i^A) + (z-y_i^A)[r(1-x^A) - (1+z-y_i^A)]} \tag{52}$$

The values of the derivatives at the inlet, i.e., at $\mathcal{A} = 0$, are obtained from

$$\left(\frac{dx^A}{dz}\right)\Big|_{\mathcal{A}=0} = \left(\frac{dx^A}{d\mathcal{A}}\right)\Big|_{\mathcal{A}=0} \Big/ \left(\frac{dz}{d\mathcal{A}}\right)\Big|_{\mathcal{A}=0} \tag{53}$$

and

$$\left(\frac{d\mathcal{A}}{dz}\right)\Big|_{\mathcal{A}=0} = 1 \Big/ \left(\frac{dz}{d\mathcal{A}}\right)\Big|_{\mathcal{A}=0} \tag{54}$$

where

$$\left(\frac{dz}{d\mathcal{A}}\right)\Big|_{\mathcal{A}=0} = -\left(\frac{dy^A}{d\mathcal{A}}\right)\Big|_{\mathcal{A}=0} \tag{55}$$

and where $(dx^A/d\mathcal{A})\,|_{\mathcal{A}=0}$ and $(dy^A/d\mathcal{A})\,|_{\mathcal{A}=0}$ are evaluated from Eqs. (24) and (23), respectively.

The following computational procedure may be used:

(1) Specify x_i^A, p_h, p_l, P^A, P^B, $L_{i(h)}$, and δ.

(2) Calculate α^*, r, and K; and y_i^A.

(3) Calculate y_i^A, (dx^A/dz), and $(d\mathcal{A}/dz)$ with the aid of Eqs. (22), (53), and (54), respectively.

(4) Initialize x^A and $\mathcal{A}$ as x_i^A and 0, respectively, then compute x^A and A as a function of z using CSMP statements; a fourth-order Runge-

Kutta method is the basis of this operation. Also, evaluate y^A from Eq. (50), and θ from the material balance and Eq. (29), or from:

$$\theta = \frac{x_i{}^A - x^A}{y_i{}^A - z - x_i{}^A} = \frac{x_i{}^A - x^A}{y^A - x^A} \tag{56}$$

(5) The computation can be terminated at any specified y^A or θ value. The computer program is presented in Appendix I.

Countercurrent Flow

CSMP was also employed in this case. A change of variable is again necessary; let

$$z = x^A - x_o{}^A \tag{57}$$

Substitution of this variable in Eqs. (46) and (47) results in:

$$\frac{dy^A}{dz} = \left(\frac{y^A - x_o{}^A}{z}\right)\left\{\frac{\begin{array}{r}(1 - y^A)\alpha^*(rz + rx_o{}^A - y^A) \\ - y^A[r(1 - z - x_o{}^A) - (1 - y^A)]\end{array}}{\begin{array}{r}(1 - z - x_o{}^A)\alpha^*(rz + rx_o{}^A - y^A) \\ - (z + x_o{}^A)[r(1 - z - x_o{}^A) - (1 - y^A)]\end{array}}\right\} \tag{58}$$

and

$$\left(\frac{d\mathcal{A}}{dz}\right) = \frac{K'[(y^A - x_o{}^A)/(z + x_o{}^A - y^A)]}{\begin{array}{r}(1 - z - x_o{}^A)\alpha^*(rz - rx_o{}^A - y^A) \\ - (z + x_o{}^A)[r(1 - z - x_o{}^A) - (1 - y^A)]\end{array}} \tag{59}$$

The value of dy^A/dz at the inlet is given by:

$$\left(\frac{dy^A}{dz}\right)\Big|_{\alpha=0} = \left(\frac{dy^A}{dx^A}\right)\Big|_{\alpha=0} = \left(\frac{dy^A}{d\mathcal{A}}\right)\Big|_{\alpha=0} \Big/ \left(\frac{dx^A}{d\mathcal{A}}\right)\Big|_{\alpha=0} \tag{60}$$

where $(dy^A/d\mathcal{A})\,|_{\alpha=0}$ and $(dx^A/d\mathcal{A})\,|_{\alpha=0}$ can be evaluated from Eqs. (44) and (45), respectively.

The computational procedure is as follows:

(1) Specify $x_i{}^A$, p_h, p_l, P^A, P^B, $L_{i(h)}$, δ, and θ.
(2) Calculate α^*, r, $L_{o(h)}$ and K'.
(3) Assume $x_o{}^A$.
(4) Calculate $y_o{}^A$ from the material balance and designate this $y_o{}^{A*}$:

$$y_o{}^{A*} = [x_i{}^A - (1 - \theta)x_o{}^A]/\theta. \tag{61}$$

(5) Calculate y_i^A and $(dy^A/dz)\,|_{\alpha=0}$ with the aid of Eqs. (43) and (60), respectively.

(6) Initialize y^A and $\mathcal{A}$ as y_i^A and 0, respectively, then compute y_o^A and $\mathcal{A}$ using CSMP statements. Compare y_o^A and y_o^{A*}. Repeat with other values of x_o^A until agreement is obtained.

This method results in a negative area, as mentioned earlier, and a sign change is therefore necessary. The computer program for this case is attached in Appendix I.

PARAMETRIC STUDIES

The separation of oxygen from air (or, more accurately, the enrichment of air in oxygen) in a single-stage permeator was studied under the same conditions as in the previous investigation (*9*). Air was assumed to be a binary gas mixture consisting of 20.9 mole-% O_2 and 79.1 mole-% N_2, and an air feed rate of 1×10^6 cm³(STP)/sec, or about 123 tons/day, was used in the calculations. It was also assumed that the separation would be effected by means of a hypothetical membrane with a permeability coefficient for oxygen, the more rapidly permeating gas, of 5×10^{-8} cm³(STP)·cm/(sec·cm²·cm Hg). This magnitude is of the same order as found for the permeation of oxygen through silicone rubber membranes at ambient temperature (*12*). The permeability coefficient for nitrogen, and, hence, the ideal separation factor α^*, was allowed to vary, with α^* taking the values 2, 5, or 10. The thickness of the membrane was taken as 2.54×10^{-3} cm (1 mil). The effect of the ratio of pressures on the two sides of the membrane, r, was not considered because it was investigated in detail in the previous study (*9*); in the present work, the condition selected was $r = 5$ with $p_h = 380$ cm Hg and $p_l = 76$ cm Hg.

The parametric calculations yielded the concentration of oxygen in the permeated and unpermeated streams leaving the stage as a function of the "stage cut" θ. The calculations were made for the cocurrent and countercurrent flow patterns discussed above, and the results were compared with the previous data for cross-flow with no mixing and for perfect mixing (*9*). The latter two flow patterns are illustrated in Fig. 4.

The results of the study are presented graphically in Figs. 5, 6, and 7. The mole-fraction of oxygen in the permeated stream leaving the stage is designated in these figures as the "oxygen enrichment," $y_o^{O_2}$. As evident from the figures, the highest enrichment is obtained for countercurrent flow, while the lowest enrichment is for perfect mixing on both

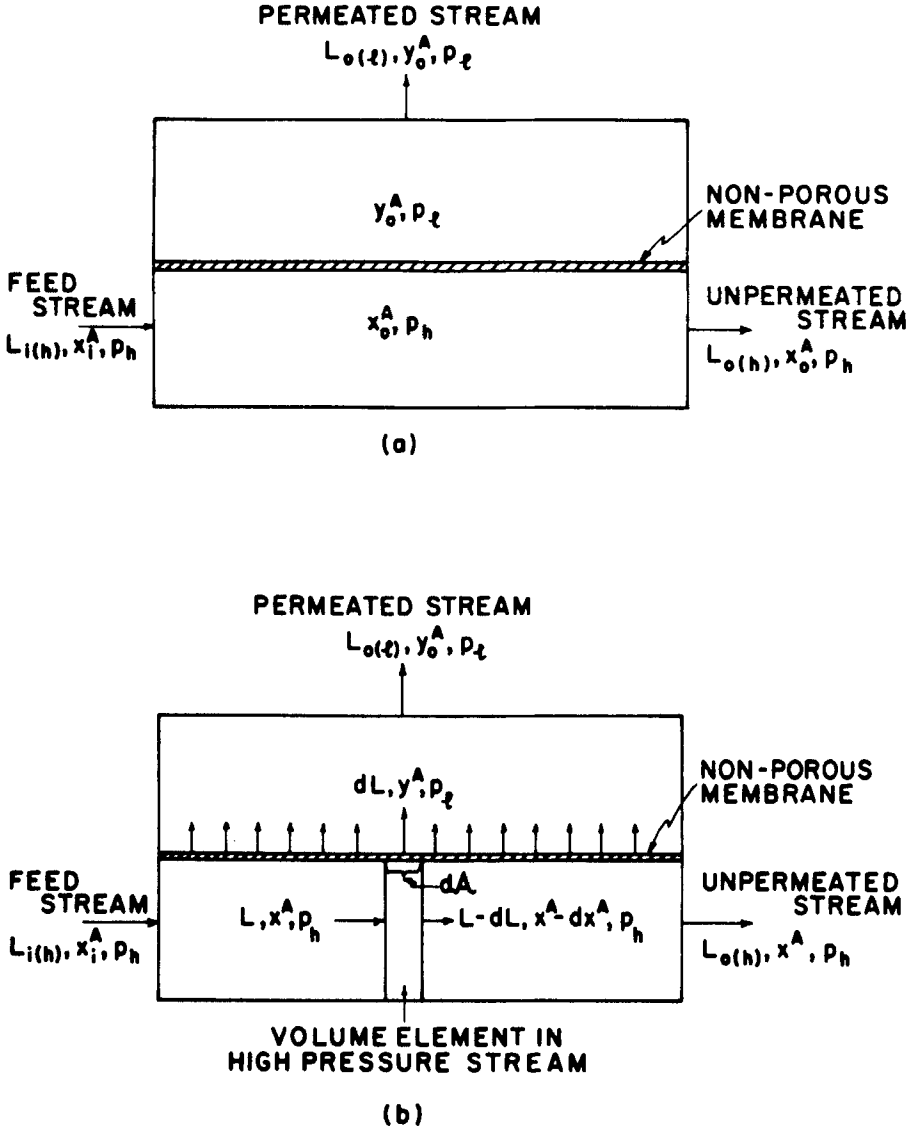

FIG. 4. Flow patterns in single permeation stage. (a) Perfect mixing on both sides of membrane. (b) Cross-flow with no mixing.

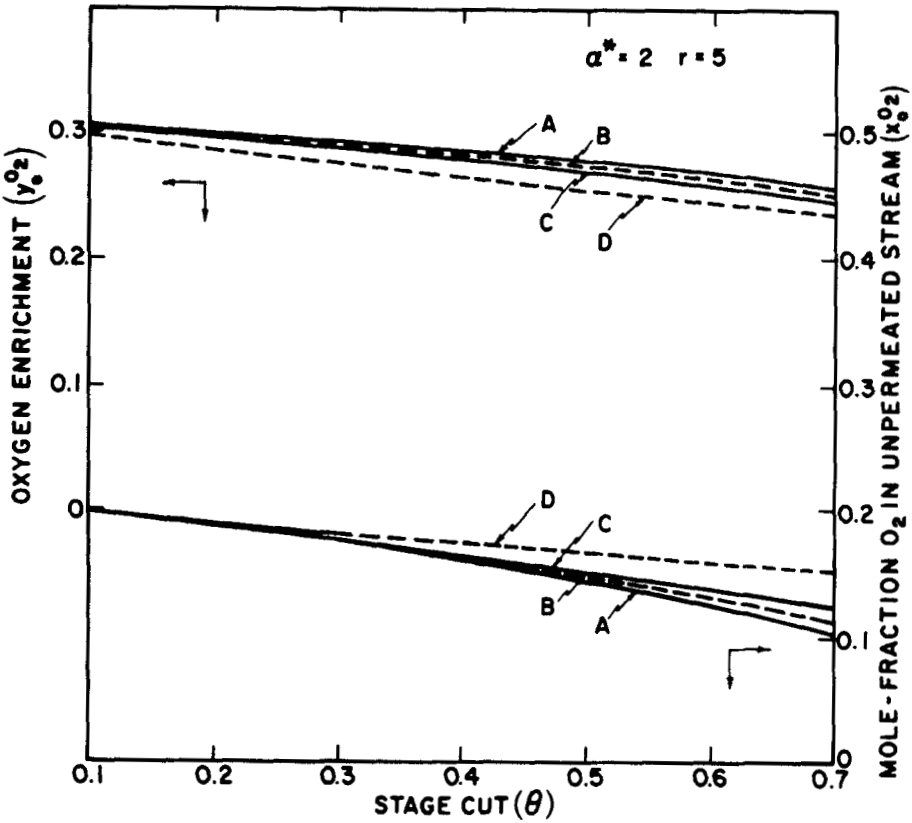

FIG. 5. Effect of flow pattern on degree of separation achievable in a single permeation stage. The figure refers to the separation of a mixture of 20.9 mole-% O_2 and 79.1 mole-% N_2, and shows the oxygen concentration (in mole fraction) in the permeated and unpermeated streams leaving the stage as a function of "stage cut." Conditions: $p_h = 380$ cm Hg; $p_l = 76$ cm Hg; $\alpha^* = 2$; $r = 5$; $P^{O_2} = 5 \times 10^{-8}$ cm³ (STP)·cm/(sec·cm²·cm Hg). A = Countercurrent flow with no mixing. B = Cross-flow with no mixing. C = Cocurrent flow with no mixing. D = Perfect mixing on both sides of membrane.

sides of the membrane. This result is expected intuitively. In comparing the effectiveness of the four flow patterns examined, it is seen that for any given "stage cut" the value of $y_o^{O_2}$ decreases in the order: $y_o^{O_2}$ (countercurrent flow) > $y_o^{O_2}$ (cross-flow with no mixing) > $y_o^{O_2}$ (cocurrent flow) > $y_o^{O_2}$ (perfect mixing). The differences in oxygen

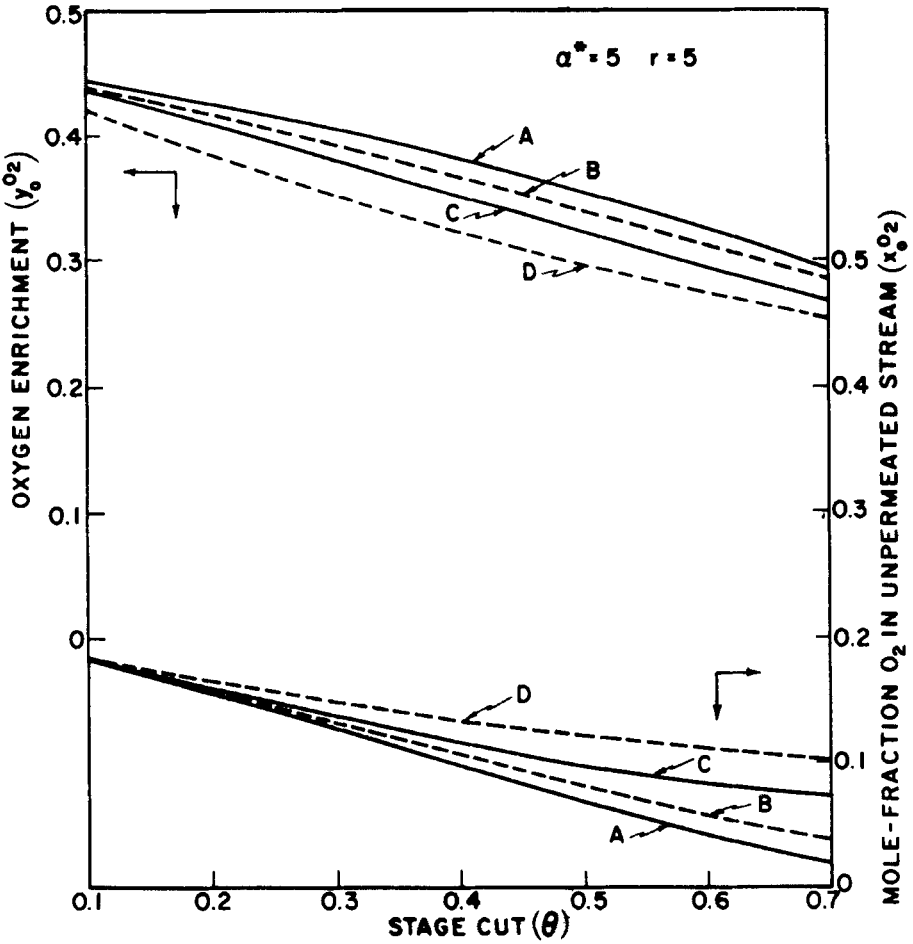

FIG. 6. Effect of flow pattern on degree of separation achievable in a single permeation stage. The figure refers to the separation of a mixture of 20.9 mole-% O_2 and 79.1 mole-% N_2, and shows the oxygen concentration (in mole fraction) in the permeated and unpermeated streams leaving the stage as a function of "stage cut." Conditions: p_h = 380 cm Hg; p_l = 76 cm Hg; α^* = 5; r = 5; $P^{O_2} = 5 \times 10^{-8}$ cm³(STP)·cm/(sec·cm²·cm Hg). A = Countercurrent flow with no mixing. B = Cross-flow with no mixing. C = Cocurrent flow with no mixing. D = Perfect mixing on both sides of membrane.

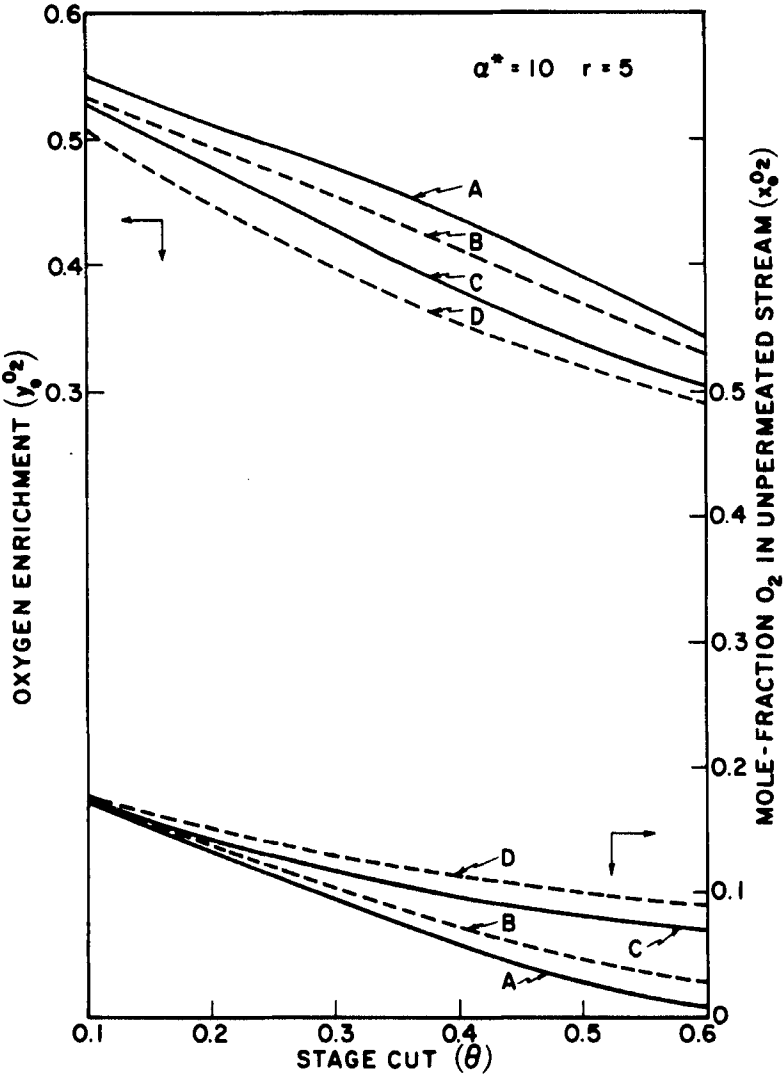

FIG. 7. Effect of flow pattern on degree of separation achievable in a single permeation stage. The figure refers to the separation of a mixture of 20.9 mole-% O_2 and 79.1 mole-% N_2, and shows the oxygen concentration (in mole fraction) in the permeated and unpermeated streams leaving the stage as a function of "stage cut." Conditions: p_h = 380 cm Hg; p_l = 76 cm Hg; α^* = 10; r = 5; $P^{O_2} = 5 \times 10^{-8}$ cm³(STP)·cm/(sec·cm²·cm Hg). A = Countercurrent flow with no mixing. B = Cross-flow with no mixing. C = Cocurrent flow with no mixing. D = Perfect mixing on both sides of membrane.

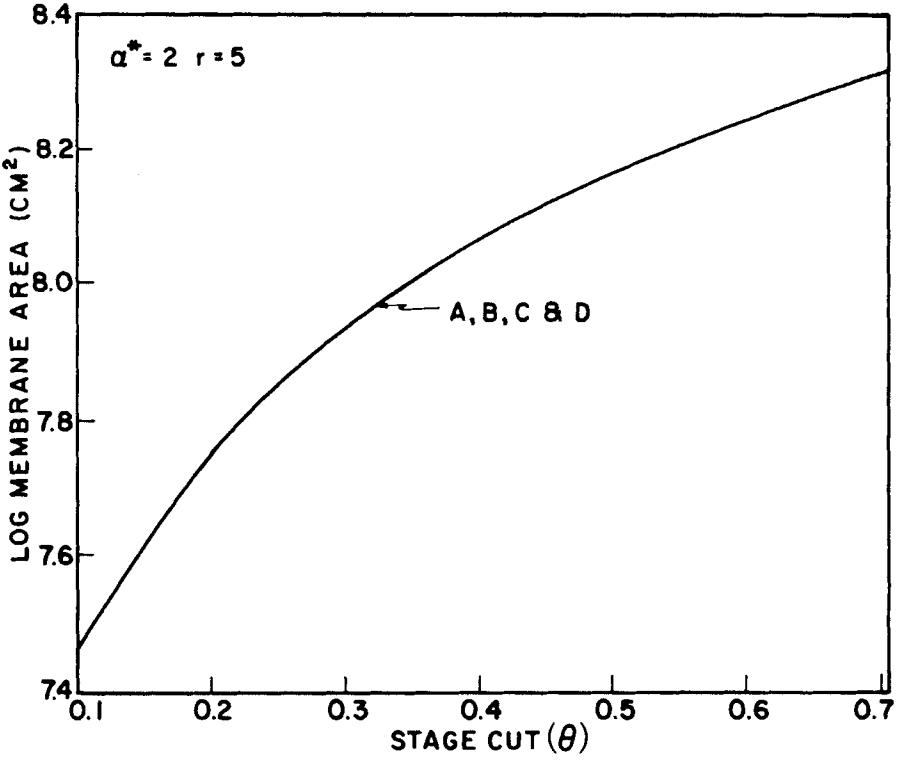

FIG. 8. Effect of flow pattern on membrane area requirement in a single permeation stage. The figure refers to the separation of a mixture of 20.9 mole-% O_2 and 79.1 mole-% N_2, and shows the membrane area requirement as a function of "stage cut." Conditions: Feed rate = 1×10^6 cm³(STP)/sec; p_h = 380 cm Hg; p_l = 76 cm Hg; $\alpha^* = 2$; $r = 5$; $P^{O_2} = 5 \times 10^{-8}$ cm³(STP)·cm/(sec·cm²·cm Hg). A = Countercurrent flow with no mixing. B = Cross-flow with no mixing. C = Cocurrent flow with no mixing. D = Perfect mixing on both sides of membrane.

enrichment between the various flow types increase with increasing ideal separation factor α^*, and the largest differences are observed for intermediate stage cuts ($0.2 < \theta < 0.6$). In the limits $\theta \to 0$ and $\theta \to 1$, the same value of $y_o^{O_2}$ is obtained at any given α^* for all flow patterns. It is interesting to note that the enrichment obtained for cross-flow approaches that for cocurrent flow at low θ's, and that for countercurrent flow for high θ's. This has been noted also by Oishi et al. (*10*). The mole-fraction

of oxygen in the unpermeated stream leaving the stage, $x_o^{O_2}$, will be lower the higher $y_o^{O_2}$, of course, because this stream is depleted in oxygen. The differences in the composition of the unpermeated stream between the various flow types also increase with increasing ideal separation factor. The greatest differences are observed at high stage cut; however, in the limit $\theta \rightarrow 1$ all curves must pass through the point $\theta = 1$, $x_o^{O_2} = 0$.

In contrast to the pronounced effect of flow pattern on oxygen enrichment, the effect on membrane area $\mathcal{A}$ is relatively slight, as shown in

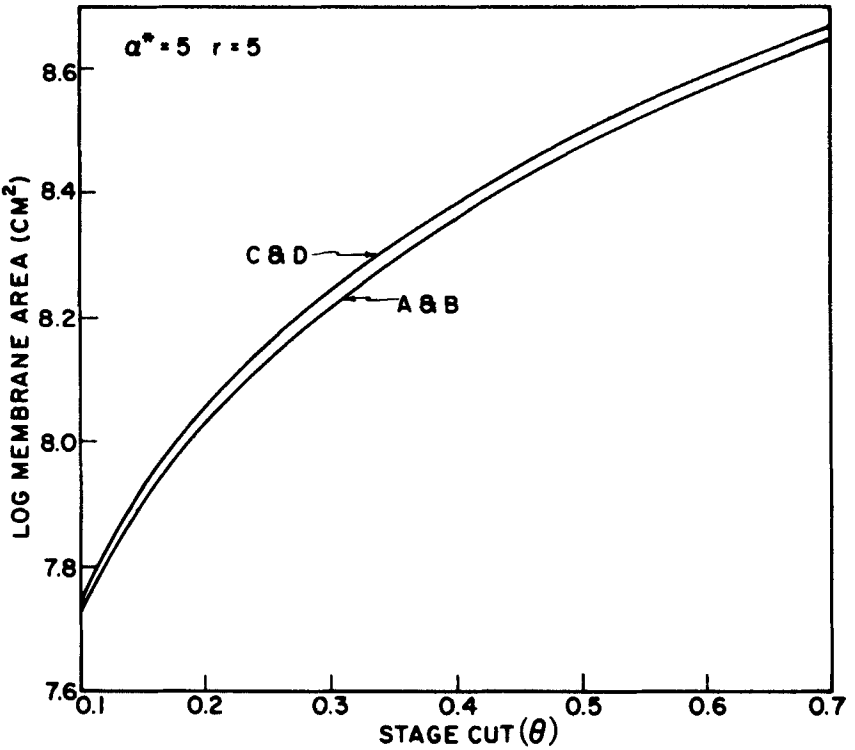

FIG. 9. Effect of flow pattern on membrane area requirement in a single permeation stage. The figure refers to the separation of a mixture of 20.9 mole-% O_2 and 79.1 mole-% N_2, and shows the membrane area requirement as a function of "stage cut." Conditions: Feed rate = 1×10^6 cm³(STP)/sec; p_h = 380 cm Hg; p_l = 76 cm Hg; $\alpha^* = 5$; $r = 5$; $P^{O_2} = 5 \times 10^{-8}$ cm³(STP)·cm/(sec·cm²·cm Hg). A = Countercurrent flow with no mixing. B = Cross-flow with no mixing. C = Cocurrent flow with no mixing. D = Perfect mixing on both sides of membrane.

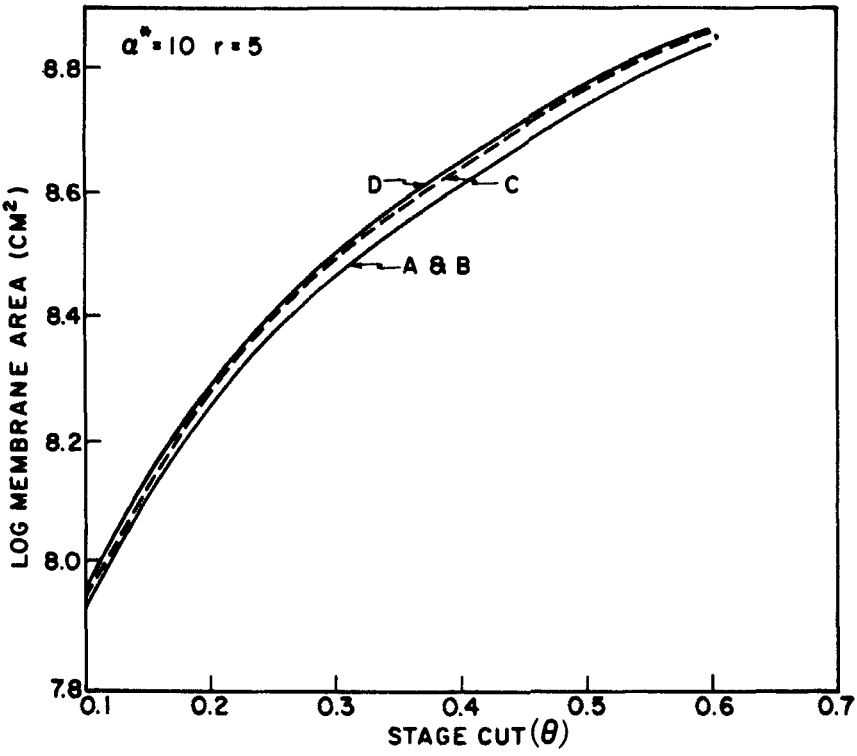

FIG. 10. Effect of flow pattern on membrane area requirement in a single permeation stage. The figure refers to the separation of a mixture of 20.9 mole-% O_2 and 79.1 mole-% N_2, and shows the membrane area requirement as a function of "stage cut." Conditions: Feed rate = 1×10^6 cm³(STP)/sec; p_h = 380 cm Hg; p_l = 76 cm Hg; $\alpha^* = 10$; $r = 5$; $P^{O_2} = 5 \times 10^{-6}$ cm³(STP)·cm/(sec·cm²·cm Hg). A = Countercurrent flow with no mixing. B = Cross-flow with no mixing. C = Cocurrent flow with no mixing. D = Perfect mixing on both sides of membrane.

Figs. 8, 9, and 10. Thus, for higher values of α^* and all stage cuts, it is observed that:

(1) $\mathcal{A}$ (countercurrent flow) $\cong \mathcal{A}$ (cross-flow), to within 1% for $\alpha^* = 5$ and 10.

(2) $\mathcal{A}$ (cocurrent flow) $\cong \mathcal{A}$ (perfect mixing), to within 1% for $\alpha^* = 5$ and 3% for $\alpha^* = 10$.

(3) $\mathcal{A}$ (countercurrent flow) $<$ $\mathcal{A}$ (perfect mixing); the difference between the two areas is 3–4% for $\alpha^* = 5$ and 10% for $\alpha^* = 10$.

At low values of α^* (for example, $\alpha^* = 2$), the membrane area requirements for a given set of operational conditions are almost independent of stage flow pattern, as reported also by Oishi et al. (*10*).

As mentioned above, the choice of countercurrent flow in the permeation stage will result in the greatest enrichment for a given $L_{i(h)}$, α^*, θ, and r. If it is desired to obtain the same enrichment by one of the other flow patterns, it is necessary to reduce the stage cut. This can be performed in two ways: (1) at a fixed product rate and membrane area, by increasing the feed rate; or (2) at a fixed feed rate, by reducing the membrane area. The first method results in a lower percentage of oxygen being recovered, or extracted, from the air feed stream and, hence, in higher operating costs. The second method, while decreasing the membrane area and, thus, the capital investment costs, results in both a lower product rate and a lower oxygen recovery.

SUMMARY AND CONCLUSIONS

The present and previous studies (*9*) have shown that:

(1) The flow pattern of the high-pressure (unpermeated) and low-pressure (permeated) streams in a permeation stage can have a significant effect on the obtainable degree of separation.

(2) The flow pattern has *relatively* little effect on the membrane area requirements, but this effect can become significant if the ideal separation factor is sufficiently large.

The achievable separation of a gas mixture in a single permeation stage depends essentially on the ideal separation factor, the ratio of pressures on the two sides of the membrane, and the flow patterns of the high-pressure and low-pressure gas streams. The membrane area, on the other hand, depends also on other factors, including the feed rate, the pressure level, the magnitude of the permeability coefficients, and the membrane thickness.

In the development of a practical permeation process it is necessary to minimize the membrane area requirements in order to reduce the capital investment costs of the process. As seen, changes in the stage flow patterns will not significantly affect the membrane area. Other alterna-

tives for reducing the membrane area are to:

(1) Decrease the membrane thickness.
(2) Increase the membrane permeability.
(3) Increase the pressure *level.*

Of these three methods, the first depends on the physical properties of the membrane and the availability of appropriate techniques for reducing the membrane thickness. Such techniques have been successfully developed in recent years, and it is now possible to produce asymmetric (Loeb-type) membranes with an effective thickness of 0.25 μ (0.01 mil) from cellulose acetate and several other polymers. The second method amounts to finding new membrane-forming polymers with higher permeabilities toward the gases of interest than those available at present. Such materials can be found at present only by trial and error. Finally, the last method depends on the overall economics of the separation process under consideration.

Acknowledgments

S.A.S. is grateful to the National Science Foundation for supporting this work under Grant No. GK-30312. W.P.W. acknowledges the partial support of the Air Force Office of Scientific Research, Office of Aerospace Research, under Contract F44620-68-0020.

APPENDIX I

Computer Programs

Cocurrent Flow

```
RENAME TIME=Z
INITIAL
AL=PA/PB
AL1=AL-1.0
R=PH/PL
B=AL1*(R*XA0+1.0)+R
C=4.0*AL*R*XA0*AL1
D=B*B-C
YA0=(B-SQRT(C))/(2.0*AL1)
E=(L*T)/(PL*PB)
GX=(AL*(R*XA0-YA0)*(XA0-YA0))/(YA0*E)
EY=(E/(XA0-YA0))-(AL1*(2.0*YA0-R*XA0-1.0)-R)/GX
```

```
GY=R*(AL-YA0*AL1)/EY
CONST   L=1.0E+6,T=2.54E-3,PA=5.0E-8
PARAM   PB=(2.5E-8,1.0E-8,5.0E-9)
PARAM   PH=152.0,PL=76.0
INCON   XA0=0.209,A0=0.0
DYNAMIC
XA1=XA0-XA
XA2=1.0-XA
Z1=AL*(R*XA+Z-YA0)
Z2=1.0+Z-YA0
Z3=R*XA2-Z2
Y1=XA2*Z1-XA*Z3
Y2=Z2*Z1+(Z-YA0)*Z3
PROCEDURE DXADZ,DADZ=BLOCK(XA1,GX,GY,XA0,YA0,XA,Z,
              Y1,Y2,E)
          IF(XA1) 1,1,2
      1   DXADZ=(-1.0)*(GX/GY)
          DADZ=(-1.0)*(1.0/GY)
          GO TO 3
      2   DXADZ=(XA1/(YA0-Z-XA0))*(Y1/Y2)
          DADZ=E*(XA1/(XA+Z-YA0))*(1.0/Y2)
      3   CONTINUE
ENDPRO
XA=INTGRL(XA0,DXADZ)
A=INTGRL(A0,DADZ)
YA=YA0-Z
THETA=XA1/(YA-XA)
AA=A+1.
LOGA=ALOG10(AA)
TERMINAL
METHOD  RKSFX
TIMER   FINTIM=1.0,DELT=0.001,PRDEL=0.001
FINISH  THETA=0.95,YA=0.209
TITLE   COCURRENT PERMEATION
PRINT   XA,YA,A,LOGA,THETA
END
PARAM   PH=380.,PL=76.
END
PARAM   PH=760.,PL=76.
END
PARAM   PH=1520.,PL=76.
END
STOP
```

Countercurrent Flow

```
RENAME  TIME=Z,FINTIM=T1
FIXED   J,K
```

```
TITLE   COUNTERCURRENT PERMEATION
INITIAL
AL=PA/PB
AL1=AL-1.0
R=PH/PL
L0=(1.0-THETA)*L
E=(L0*T)/(PL*PB)
        YA1=(XA0-(1.0-THETA)*X0)/THETA
CONST   L=1.0E+6,T=2.54E-3,PA=5.0E-8
CONST   X0=0.01
CONST   H=0.01
PARAM   PH=380.0,PL=76.0
PARAM   PB=5.0E-9
CONST   K=0,J=0
INCON   XA0=0.209,A0=0.0
PARAM   THETA=0.6
        T1=XA0-X0
        B=AL1*(R*X0+1.0)+R
        C=4.0*AL*R*X0*AL1
        D=B*B-C
        YA0=(B-SQRT(D))/(2.0*AL1)
        GX=(AL*(R*X0-YA0)*(X0-YA0))/(YA0*E)
        EY=(E/(X0-YA0))-(AL1*(2.0*YA0-R*X0-1.0)-R)/GX
        GY=R*(AL-YA0*AL1)/EY
DYNAMIC
        XA2=1.0-X0-Z
        Z1=AL*(R*Z+R*X0-YA)
        Z2=R*(1.0-Z-X0)
        Z3=1.0-YA
        Z4=Z2-Z3
        Y1=Z3*Z1-YA*Z4
        Y2=XA2*Z1-(Z+X0)*Z4
PROCEDURE  DYADZ,DADZ=BLOCK(GX,GY,YA,X0,Z,Y1,Y2,E)
        IF(Z)30,20,30
   20   DYADZ=GY/GX
        DADZ=1.0/GX
        GO TO 40
   30   DYADZ=((YA-X0)/Z)*(Y1/Y2)
        DADZ=(E*(YA-X0)/(Z+X0-YA))*(1.0/Y2)
   40   CONTINUE
ENDPRO
        YA=INTGRL(YA0,DYADZ)
        AN=INTGRL(A0,DADZ)
        X1=X0+Z
        A=-AN
        LOGA=ALOG10(A+1.0)
        DIF=ABS(YA1-YA)
```

```
TERMINAL
          IF(J-1)42,42,95
      42  TEST=ABS(YA1-YA)
          IF(K)45,50,45
      45  IF(TEST-TEMP)50,50,60
      50  TEMP=TEST
      60  X0=X0+H
          IF(X0.GE.0.209) GO TO 65
          K=K+1
          IF(K-20)90,65,65
      65  IF(J-1)70,75,75
      70  X0=XA-H
          H=H/10.
          K=0
          J=J+1
          IF(X0.GT.0.0) GO TO 90
          X0=X0+H
          K=1
          GO TO 90
      75  X0=XA
          J=J+1
          GO TO 95
      90  CALL RERUN
      95  CONTINUE
          METHOD RKSFX
          TIMER DELT=0.001,T1=0.199
          END
TIMER     PRDEL=0.001
PRINT     X0,THETA,X1,YA,A,LOGA,DIF
END
STOP
```


APPENDIX II

Perfect Mixing in the Permeation Stage

Certain results of the parametric study on air separation reported in the previous work were presented in tabular form (*9*). These tables were inadvertently labeled as pertaining to perfect mixing conditions on both sides of the membrane, whereas they referred, in fact, to cross-flow with no mixing. The correct results for perfect mixing are presented in the Tables 1–4. None of the previous conclusions is affected by this correction. Reference is also made to Eqs. (21), (22), (44), and (45) of the

TABLE 1

Effect of Ideal Separation Factor on Membrane Area and Oxygen Enrichment. Perfect Mixing in High-Pressure and Low-Pressure Streams[a]

Stage cut (θ)	Membrane area ($cm^2 \times 10^{-8}$)				Enrichment (mole-fraction, y_{O_2})			
	$\alpha^*=2$	$\alpha^*=5$	$\alpha^*=10$	$\alpha^*=100$	$\alpha^*=2$	$\alpha^*=5$	$\alpha^*=10$	$\alpha^*=100$
0.1	0.494	0.917	1.40	4.41	0.312	0.467	0.581	0.858
0.2	0.996	1.94	3.18	18.5	0.297	0.421	0.507	0.690
0.3	1.51	3.05	5.29	40.4	0.284	0.379	0.441	0.545
0.4	2.02	4.24	7.64	65.4	0.271	0.343	0.385	0.445
0.5	2.55	5.49	10.1	91.9	0.259	0.312	0.340	0.375
0.6	3.08	6.77	12.8	119.2	0.247	0.285	0.303	0.329
0.7	3.61	8.09	15.4	147.0	0.237	0.262	0.273	0.285
0.8	4.15	9.45	18.2	175.1	0.227	0.242	0.248	0.254
0.9	4.69	10.8	20.9	203.4	0.218	0.224	0.227	0.229

[a] Pressure ratio $r = 10$; low pressure $p_l = 19$ cm Hg.

TABLE 2

Effect of Ideal Separation Factor on Membrane Area and Oxygen Enrichment. Perfect Mixing in High-Pressure and Low-Pressure Streams[a]

Stage cut (θ)	Membrane area ($cm^2 \times 10^{-8}$)			Enrichment (mole-fraction, y_{O_2})		
	$\alpha^* = 2$	$\alpha^* = 5$	$\alpha^* = 10$	$\alpha^* = 2$	$\alpha^* = 5$	$\alpha^* = 10$
0.1	0.280	0.546	0.895	0.297	0.421	0.507
0.2	0.564	1.14	1.96	0.285	0.384	0.447
0.3	0.852	1.77	3.17	0.273	0.351	0.397
0.4	1.14	2.44	4.48	0.262	0.322	0.354
0.5	1.44	3.14	5.87	0.252	0.297	0.319
0.6	1.73	3.85	7.30	0.242	0.274	0.289
0.7	2.03	4.58	8.78	0.233	0.255	0.264
0.8	2.34	5.33	10.3	0.225	0.238	0.243
0.9	2.64	6.08	11.8	0.217	0.222	0.225

[a] Pressure ratio $r = 5$; low pressure $p_l = 76$ cm Hg.

TABLE 3

Effect of Pressure Ratio on Membrane Area and Oxygen Enrichment for Constant High Pressure. Perfect Mixing in High-Pressure and Low-Pressure Streams[a]

Stage cut (θ)	Membrane area ($cm^2 \times 10^{-8}$)				Enrichment (mole-fraction, y_{O_2})			
	$r = 2$	$r = 5$	$r = 10$	$r = 20$	$r = 2$	$r = 5$	$r = 10$	$r = 20$
0.1	0.987	0.546	0.458	0.421	0.312	0.421	0.466	0.490
0.2	2.01	1.14	0.970	0.897	0.297	0.384	0.421	0.440
0.3	3.06	1.77	1.52	1.42	0.282	0.351	0.379	0.395
0.4	4.13	2.44	2.12	1.98	0.269	0.322	0.343	0.355
0.5	5.26	3.14	2.74	2.58	0.257	0.297	0.312	0.320
0.6	6.34	3.85	3.39	3.19	0.246	0.274	0.285	0.291
0.7	7.47	4.58	4.05	3.82	0.236	0.255	0.262	0.265
0.8	8.62	5.33	4.72	4.46	0.226	0.238	0.242	0.244
0.9	9.78	6.08	5.40	5.11	0.217	0.222	0.224	0.225

[a] Ideal separation factor $\alpha^* = 5$; high pressure $p_h = 380$ cm Hg.

TABLE 4

Effect of Pressure Ratio on Membrane Area and Oxygen Enrichment for Constant Low Pressure. Perfect Mixing in High-Pressure and Low-Pressure Streams[a]

Stage cut (θ)	Membrane area ($cm^2 \times 10^{-8}$)				Enrichment (mole-fraction, y_{O_2})			
	$r = 2$	$r = 5$	$r = 10$	$r = 20$	$r = 2$	$r = 5$	$r = 10$	$r = 20$
0.1	4.57	0.895	0.349	0.153	0.340	0.507	0.581	0.619
0.2	9.38	1.96	0.795	0.356	0.319	0.447	0.507	0.539
0.3	14.4	3.17	1.32	0.604	0.299	0.397	0.441	0.465
0.4	19.6	4.48	1.91	0.883	0.282	0.354	0.385	0.402
0.5	25.0	5.87	2.54	1.18	0.267	0.319	0.340	0.352
0.6	30.5	7.30	3.19	1.50	0.253	0.289	0.303	0.311
0.7	36.1	8.78	3.86	1.82	0.240	0.264	0.273	0.278
0.8	41.8	10.3	4.54	2.15	0.229	0.243	0.248	0.250
0.9	47.6	11.8	5.24	2.48	0.219	0.225	0.227	0.228

[a] Ideal separation factor $\alpha^* = 10$; low pressure $p_l = 76$ cm Hg.

above-mentioned study (*9*); the term on the left-hand side of these equations should have a (−) sign.

REFERENCES

1. K. Cohen, *The Theory of Isotope Separation*, National Nuclear Energy Series, Division III, Vol. IB, McGraw-Hill, New York 1957.
2. S. Weller and W. A. Steiner, *J. Appl. Phys.*, *21*, 279 (1950).
3. S. Weller and W. A. Steiner, *Chem. Eng. Progr.*, *46*, 585 (1950).
4. H. E. Huckins and K. Kammermeyer, *Chem. Eng. Progr.*, *49*, 180 (1953); *Ibid.*, *49*, 295 (1953).
5. D. W. Brubaker and K. Kammermeyer, *Ind. Eng. Chem.*, *46*, 733 (1954).
6. R. W. Naylor and P. O. Backer, *Amer. Inst. Chem. Eng. J.*, *1*, 95 (1955).
7. M. E. Brewer and K. Kammermeyer, *Separ. Sci.*, *2*, 319 (1967).
8. S. A. Stern, T. F. Sinclair, P. J. Gareis, N. P. Vahldieck, and P. H. Mohr, *Ind. Eng. Chem.*, *57*, 49 (1965).
9. S. A. Stern and W. P. Walawender, Jr., *Separ. Sci.*, *4*, 129 (1969).
10. J. Oishi, Y. Matsumura, K. Higashi, and C. Ike, *J. At. Energy Soc. Japan*, *3*, 923 (1961); U.S. Atomic Energy Commission Report AEC-TR-5134.
11. IBM Manual H 20-0367-3 *System/360 Continuous System Modeling Program User's Manual*, 4th ed., October 1969.
12. K. Kammermeyer, *Ind. Eng. Chem.*, *49*, 1685 (1957).

Received by editor December 27, 1971